# Acoustic characterization of ceramic $Al_2O_3$/MgO samples produced via unidirectional freeze-casting

**T.S.da N. Guenka** [1], **M.R. Machado** [1], **A.M.A. Silva** [1], **M.A.A. Nunes** [2]
[1] UnB, Campus Universitário Darcy Ribeiro, Department of Mechanical Engineering,
Asa Norte, Brasília-DF, CEP 70910-900, Brazil
e-mail: **tome.guenka@aluno.unb.br**

[2] UnB, Faculdade UnB Gama - FGA, Department of Automotive Engineering,
Área Especial de Indústria Projeção A, Setor Leste, Gama, CEP 72.444-240, Brazil

## Abstract
Aiming at an investigation of sound propagation through samples via freeze-casting, $Al_2O_3$ (corundum)/$MgO$ (periclase) monoliths were fabricated and its sound absorption properties were investigated. Using impedance tube testing, the acoustic surface impedances and absorption coefficients were measured for the produced porous monoliths. To properly understand the influence of the obtained microstructural and mechanical characteristics on the noise reduction features of these samples, the Johson-Champoux-Allard-Lafarge (JCAL) model parameters were estimated using inverse parameter identification utilizing the obtained values for surface impedance. The Found JCAL parameters are then related to the sample's microstructure, which are analyzed using Scanning Electron Microscopy (SEM) and Archimedes principle. Results show discrepancies between the obtained acoustical properties and the evaluated microstructure.

## 1 Introduction

With noise control becoming increasingly important in the most diverse fields of application among engineering solutions, new specific, complex necessities and conditions arise that are to be fulfilled simultaneously to the noise control specifications. Moreover, solutions for a specific problem that happen to tackle another (or many others) difficulty associated with the project are always welcome.

One common path chosen for noise control in a wide range of applications is the use of porous sound absorbing materials, for instance polyurethane (PU) foams and fibrous materials. These materials, though, are usually sensible to a variety of environmental circumstances, e.g. thermal shock, chemically aggressive atmospheres and mechanical abrasion - hampering its possibility of successful and prolonged usage. Nevertheless, porous materials not generally used for sound absorption such as metalic foams or macroporous ceramics have been shown to have valuable properties including low density associated with decent mechanical properties [1] [2], and have also been researched for sound absorption [3] [4] showing good results.

Focusing on macroporous ceramics, besides the vast amount of ceramics that may be used, there are different methods for its fabrication [2]. These different routes and materials result in different pore morphologies and porosities, consequently resulting in different sound absorption capabilities. Du et al. [5] used direct foaming method to obtain highly porous (more than 80 %) silica ceramic foams reaching upwards of 0.8 absorption coefficient for given raw material compositions, with mechanical strength and sound absorption characteristics being dependent on such composition. Yan et al. [6] produced ZrC ceramics via evaporating solvent and hot-pressing, developing a method that allowed porosity and pore size control, both characteristics that were then correlated to the sound absorption characteristics. He et al. [7] studied porous ceramic previously produced via twice foaming coated with a graphene oxide/styrene- butadiene rubber composite. They obtained an increase in the low frequency (200 Hz-800 Hz) sound absorption in relation to the uncoated samples, an

improvement, according to the authors, probably related to the increased tortuosity, viscoelastic damping and inter-layer dissipation brought by composite coating. Du et al, [8] prepared porous silica samples via freeze-casting method, using TBA as solvent, controlling freezing temperature and solid content to obtain different porosities and pore sizes. The acoustic characterization found that the smaller pore size resulted in overall better absorption, the same for higher porosity.

Similarly, we produced $Al_2O_3$ (alumina)/$MgO$ (Magnesium oxide) porous samples using the freeze-casting method with camphene as solvent. The freeze-casting method allows for the controlled creation of open connected porous structures for various different class materials, with different types of solvents, through the freezing of the suspension [9] [10]. Solid concentration and speed of the moving freeze front are examples of preponderant process parameters for the connectivity and geometry of the generated pores [11] [12]. Such porous structures have numerous possible applications, one of which being the acoustic absorption [8] . Camphene has been widely used for freeze-casting fabrication given that it can be frozen and sublimed at room temperature [13] [14], avoiding the need for complex freezing process.

The samples were prepared using a determined concentration of the two solid components while maintaining the solid content of the slurry. Acoustic properties are found using impedance tube testing and the obtained surface impedance curves are used to obtain the structural parameters of the Johson-Champoux-Allard-Lafarge (JCAL) model through curve fitting. The microstructural characteristics are also investigated for the samples using a Scanning Electron Microscope (SEM) and their correlation to the JCAL parameters is discussed.

# 2 Methodology

## 2.1 Freeze-Casting

The freeze-casting process consists on the preparation of a slurry containing the solid components of the sample dispersed in a solvent. Such slurry is then frozen by an externally applied temperature gradient. The nucleation of solid crystals generates a freezing front that pushes the solid content, creating a structure consisting of connected solid solvent crystals with agglomerated solid content in between such crystals. Then, the solvent is sublimated and the remaining structure, consisting of a replica of the solidified solvent, is subsequently sintered [9].

For the monoliths production, the used starting powders were CT3000SG $\alpha$-$Al_2O_3$ (99.8 wt %/ Almatis Brazil) and Magnesium Oxide ( $\geq$ 99 % trace metals basis, -325 mesh, Sigma Aldrich). The used dispersant was Texaphor 963 (Cognis, Southampton Hampshire, UK) and the solvent was camphene ( 95 wt% /Sigma Aldrich). Initially, a solution containing camphene and Texaphor was prepared at $60^\circ$ C inside a closed vessel to keep the camphene loss due to evaporation to a minimum. After verifying full dissolution of the dispersant in the solvent, alumina was added under vigorous stirring. Once the alumina powder was sufficiently dispersed, maintaining the stirring, magnesia was added. To promote adequate dispersion of both solid components in the solvent, the solution was kept under stirring for an additional 15 minutes after the inclusion of both solid components.

After mixing, the suspension was poured inside a pre-heated PTFE mold on the top of a refrigerated copper plate. The plate is U shaped and was partially immersed on liquid nitrogen to maintain its temperature. This unidirectional cooling has been shown to propitiate a unidirectional solidification, promoting an alignment of pore channels parallel to freezing front [15]. Following complete solidification, the slurry was demolded and left resting for seven days in open air for the complete camphene sublimation. After the sublimation, the green bodies were then sintered at $1300^\circ$C for 2 hours, with a heating rate of $5^\circ$C.

## 2.2 Acoustic impedance model

To model the acoustic properties of the ceramic samples, the semi phenomenological JCAL model was used. Originally proposed to describe the complex equivalent fluid density of a rigid (motionless), isotropic porous

material, the model proposed by Johnson et al. [16] was then complemented with the model by Champoux and Allard [17] that further elaborated the equivalent bulk modulus dependence on frequency for the same materials. Finally, Lafarge et al. [18] suggested changes to bulk modulus equation in order to correct lacking description of low-frequency thermal phenomena in the previous models, leading to the JCAL model. A complete description of the model may be found in [19].

The equations for the equivalent density and bulk modulus, both functions of sound frequency $\omega$, are given as:

$$\rho_{eq}(\omega) = \frac{\rho_f \alpha_\infty}{\phi}\left[1 - \frac{\nu_f \phi}{\omega k_0 \alpha_\infty}\sqrt{1 + i\frac{\omega}{\nu_f}\left(\frac{2\alpha_\infty k_0}{\phi\Lambda}\right)^2}\right] \tag{1}$$

$$K_{eq}(\omega) = \frac{\gamma P_0}{\phi}\left\{\frac{\gamma(\gamma-1)}{1 - i\frac{\phi\nu'_f}{\omega k'_0}\sqrt{\frac{i\omega}{\nu'_f}\left(\frac{2k'_0}{\Lambda'\phi}\right)^2 + 1}}\right\}^{-1}. \tag{2}$$

In equations 1 and 2, $P_0$ is the atmosferic pressure, $\rho_f$ is the saturating fluid density, $\gamma$ is its specific heat ratio, $\nu_f$ its kinematic viscosity and $\nu'_f$ is defined as $\nu_f/\text{Pr}$, where Pr is the Prandtl number. In addition to the saturating fluid properties, the JCAL model is based on 6 geometrical parameters of the porous medium, specific to the pore morphology. These are the open porosity $\phi$ , the tortuosity $\alpha_\infty$, static viscous permeability $k_0$, static thermal permeability $k'_0$ and the viscous and thermal characteristic lengths $\Lambda$ and $\Lambda'$, respectively.

From the equivalent fluid properties, its characteristic impedance $Z_c$ and the its complex wave number $k$ are obtained:

$$Z_c = \sqrt{(K_{eq}\rho_{eq})}, \tag{3}$$

$$k = \sqrt{\omega(\rho_{eq}/K_{eq})}. \tag{4}$$

Finally, from equations 3 and 4 it is possible to determine the surface impedance of a sample with thickness $d$:

$$Z = -i\frac{Z_c}{\phi}\text{cotg}(kd). \tag{5}$$

Using the surface impedance of the sample, the reflection coefficient $r$ of the sample is determined and the sample acoustic absorption $\alpha$ can be acquired:

$$r(\omega) = \frac{Z(\omega) - Z_f}{Z(\omega) + Z_f}, \tag{6}$$

$$\alpha = 1 - |r|^2. \tag{7}$$

The geometrical parameters from the JCAL model are based on average pore morphology. They can be measured directly with experimental techniques, as detailed and reported in [16] [17] [18] [19], or using multiscale models that aim to recreate the pore characteristics using idealized Periodic Unit Cells (PUC) or Representative Element Volumes (REV) based on the material structure and, via simulation and numerical calculations, obtain approximate parameter values [20] [21] . Another possible approach is the inverse characterization of the material, which is used in the present paper.

Inverse characterization is the estimation of the model parameters using an inverse problem/optimization approach [22]. For this purpose, a suitable objective function based on one of a sample's measured acoustic

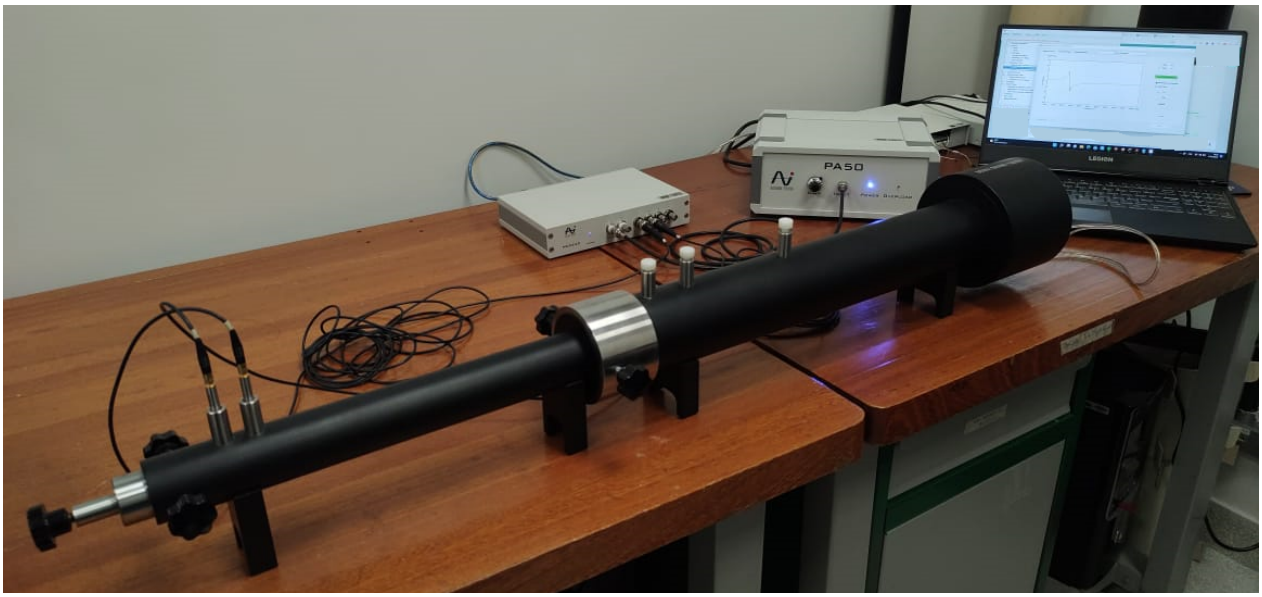


Figure 1: Acoustic characterization equipment

property (e.g. surface impedance [22] [23], reflection [24] or absorption coefficient [25]) is defined and minimized. Once a convergence criterion for the minimization process is achieved, the parameters estimates are obtained. The used objective function is:

$$R(\mathbf{a}) = 0.5 \sum_{\omega} |Z^{exp}(\omega) - Z(\omega, \mathbf{a})|, \tag{8}$$

where $Z^{exp}(\omega)$ is the obtained experimental sample surface impedance at frequency $\omega$, $Z(\omega, \mathbf{a})$ is the obtained modeled surface impedance for the vector of model parameters $\mathbf{a}$ at the same frequency. Notice that the objective function only uses data points obtained for different frequencies, without using other possible setups that can increase the size of the dataset such as different air gaps [23] [26] or incidence angles [24], simply due to equipment limitations.

There are different numerical optimization methods available for solution of the problem, many already implemented in commercial or open-source packages. A version of the Levenberg-Marquardt [27] [28] algorithm was implemented and the parametric version of the JCAL model presented in [23] was used as the numerical surface impedance model for the samples.

## 2.3 Acoustic characterization

For the experimental acoustic characterization of the samples, the BWSA SW466 impedance tubes were used, consisting of two tubes of different internal diameter: one with 30 mm and another with 60 mm internal diameter. The smaller tube is used for higher frequencies, with a range of 1000-6300 Hz, while the larger yields results for lower frequencies from 100 Hz - 2500 Hz. A MC3242 data acquisition board coupled to the PA 50 amplifier and two microphones were used. Additionally, the employed VA-Lab4 software generates the signal for the sound source and also gives the acquired results for acoustic impedance, absorption and reflection coefficients, based on transfer function method described in ISO 10534:2. Figure 1 shows the impedance tube setup.

The production of $\varnothing = 60$ mm samples using the freeze-casting method is very resource demanding considering the amount of suspension necessary to fill the mold for such samples. Moreover, recreating the freezing step parameters of a $\varnothing = 30$ mm sample for a $\varnothing = 60$ mm sample would be very difficult given the difference in temperature distribution on the cold plate due to the different base area of the molds and also the amount of slurry being solidified, among other factors. The confection of both kinds of samples

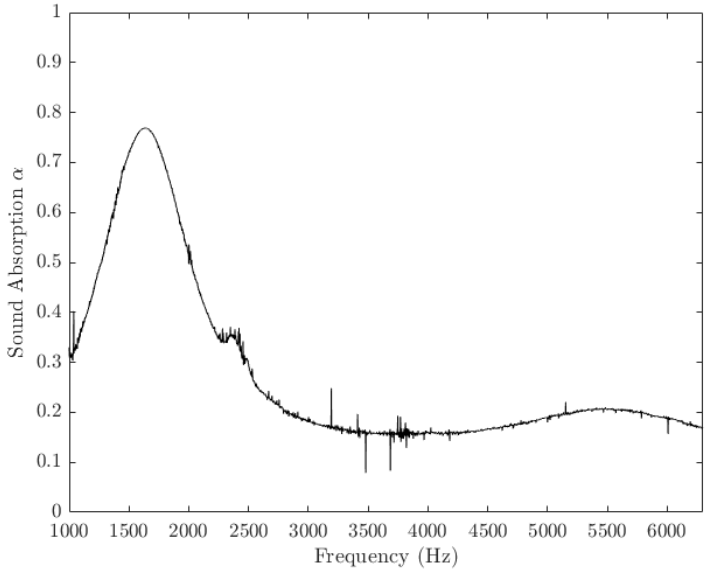


Figure 2: The acoustic absorption coefficient of the sample

using this method then would likely result in samples with, in addition to different diameters, different pore morphologies and thus different acoustic properties.

# 3 Results and Discussion

## 3.1 Inverse Characterization of the Monolith

Two samples were produced with initial concentrations shown in Table 1. During sintering phase, one of the final samples cracked, likely due to temperature gradient during cooling, and could not be reliably used for characterization. Then, the following results show the characteristics of the extracted sample, that was sanded to fit the $\varnothing = 30$ mm sample holder and had $h = 20$ mm height. The experimentally obtained acoustic absorption coefficient $\alpha$ of the sample is shown in Figure 2. It can be observed that the absorption curve is not smooth, with a pronounced $\alpha = 0.78$ absorption peak around 1700 Hz and low absorption for the rest of the evaluated frequencies.

Table 1: Fabrication specifications of the characterized sample

| Solvent concentration | Solid Concentration | Dispersant concentration |
|---|---|---|
| 80 vol% Camphene/ 20 vol% solid | 72 wt% $Al_2O_3$/28 wt% MgO | 2 wt% solid mass |

Inverse characterization of the sample following the JCAL model was performed using the obtained surface impedance given by the VALab software based on the atmospheric conditions and obtained specific impedance ratio. The used scaling frequencies required by the used parametric equations proposed in [23] were $f_* = 1200$ Hz and $f_*^{'} = 3000$ Hz. The real and imaginary parts of the acquired surface impedance ratio to the air impedance and the final fits of the inverse characterization are shown in Figure 3.

It can be seen from both Fig. 3a and 3b that the surface impedance ratio values are very high compared to other sound absorbing materials (e.g. those evaluated in [22] and [23]). Such high impedance values were detrimental to the solution of the inverse characterization algorithm, often resulting in local minimum values of the objective function, inconsistent parameter values (e.g. negative values or $\lambda > \lambda^{'}$) and overall excessive sensibility to initial guests. These hindrances may be partially explained by the used Levenberg-Marquardt

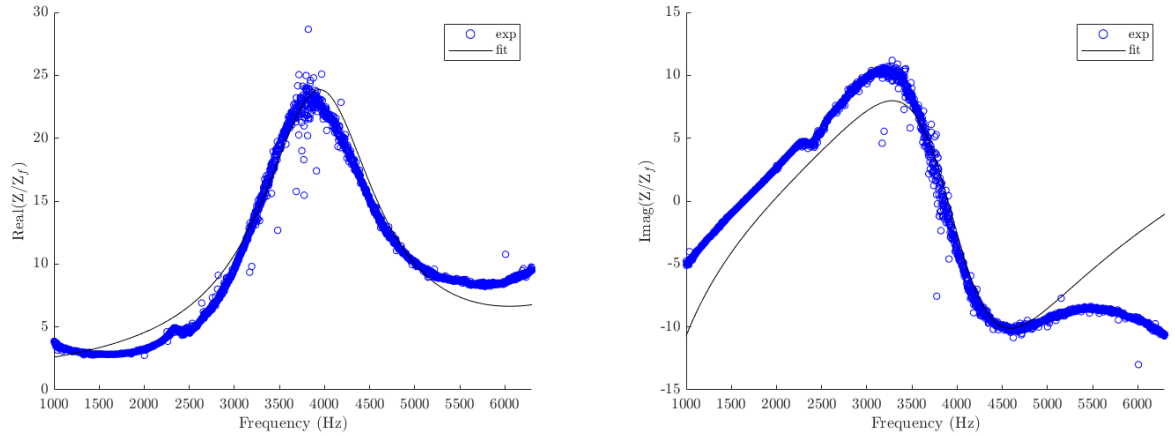


(a) (b)

Figure 3: The real and imaginary parts of the obtained sample surface impedance

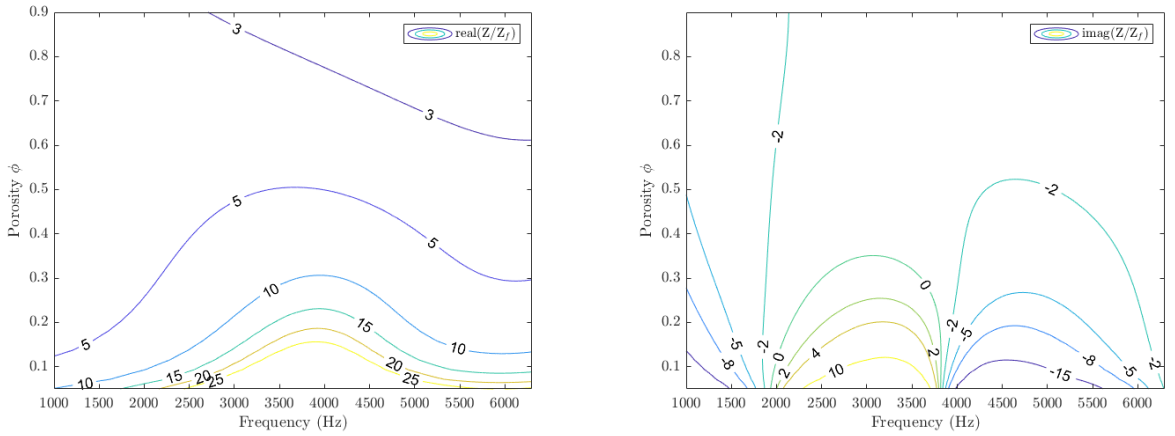


(a) (b)

Figure 4: Contour plots of the real and imaginary parts of the impedance ratio.

algorithm limitations and inherent behavior, for instance the impossibility of establishing parameter upper or lower boundaries.

Given these high acoustic impedances, a brief investigation was conducted on the reason for such observed values in an attempt to improve the parameter inversion. It was found that this measured impedances were signaling a low porosity, as shown by the contour plots in Figure 4 which present the impedance ratios varying as function of the open porosity with all other parameters kept constant with values $k_0 = 9,005\text{e}{-11}$,$k_0^{'} = 9\text{e}{-8}$,$\lambda = 6,7\text{e}{-5}$,$\lambda^{'} = 1,3\text{e}{-3}$ and $\alpha_\infty = 3$.

The initial parameter values guesses were then modified to have a low porosity value. Although better results were obtained, the obtained parameters were still either incoherent or were not an appropriate fit of the curves. Finally, by using the available interactive JCAL model plotter available in [29], the initial guesses were improved and finally coherent and good fits were obtained, with final obtained parameter values shown in Table 2.

## 3.2 Material characterization

Scanning electron microscope (SEM) images were obtained to verify the pore morphology resulting from the freeze-casting process. These images were taken from a cleaved sample, around the central (mid height and

Table 2: Sample‘s numerically found acoustic properties.

| sample | $\phi$ | $\alpha_\infty$ | $\lambda$ (m) | $\lambda_p$ (m) | $k_0$ (m$^2$) | $k_0^{'}$ (m$^2$) |
|---|---|---|---|---|---|---|
| 72 wt% Al2O3/28 wt% MgO | 0,1819 | 2,8964 | 6,752e-5 | 1,3232e-3 | 7,2971e-10 | 9,4139e-8 |

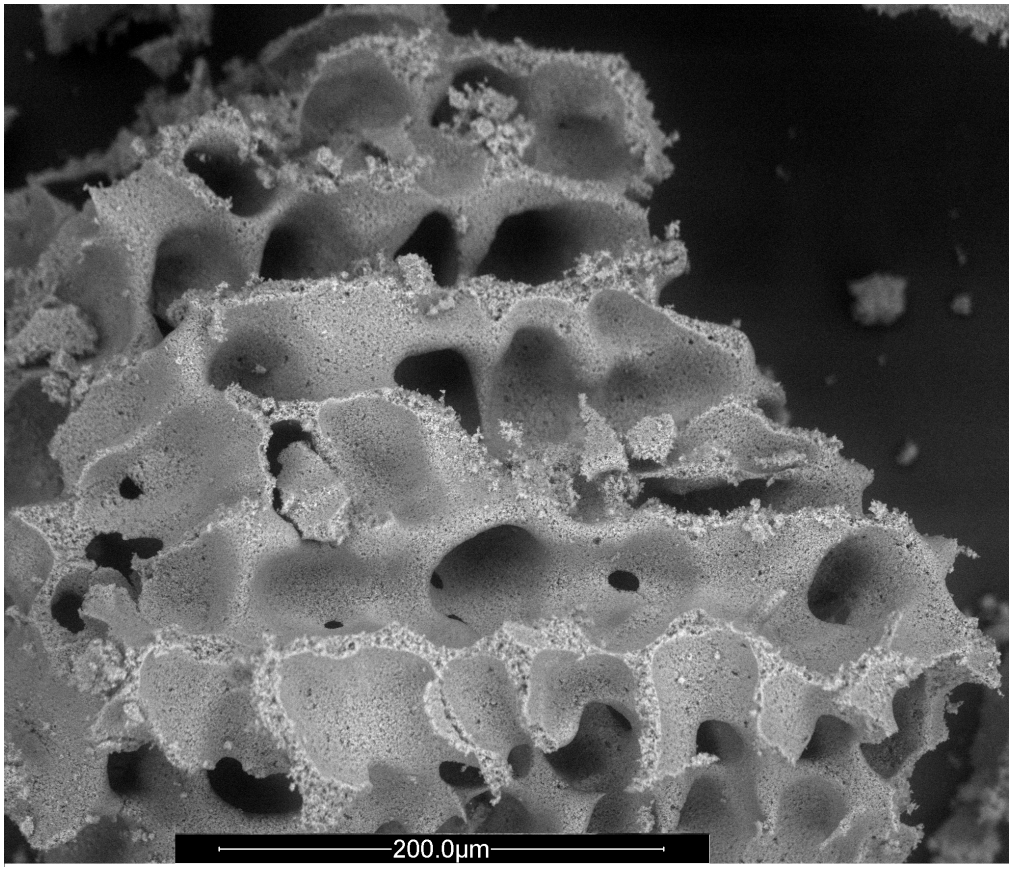


Figure 5: SEM image of the sample porous structure

mid radius) region of the cleaved surface. Unfortunately, due to limitations in equipment and mishandling of the sample, additional better quality images of the sample were not obtained. Figure 5 shows the surface image of one of the samples.

Interconnected, elongated aligned pores can be seen from the image, showing that the unidirectional freezing had effect in promoting such structure. The pores can be said to have the shape of non-uniform cylinders, with irregular windows that may connect to other cylindrical pores. It is in general, a highly irregular structure, in spite of the observed aligment of the pores. The lack of additional quality images prevents the analysis of an average pore/window size, although it can be seen that the average pore width is around 50 $\mu$m, thus rendering the found $\lambda^{'}$ value to be around 40 times higher than the pore radius $\approx 2\lambda^{'}$ estimation.

Besides SEM, Archimedes principle was used to obtain an estimate of the open porosity of the sample. The calculated open porosity was found to be 63,79 %, contrasting radically to the found acoustic porosity. Such discrepancy can have various explanations. One possibility is the graded porosity of samples made via freeze-casting reported in studies with solvent, starting powders and freezing conditions very similar to those used in the present paper [30] (and also others not so similar [31]), in which the top and bottom of the samples have a dense layer due to the suspension quickly freezing in these regions - this dense layer may hamper the propagation of sound through the studied sample, if present. Also relating to the characteristic lengths, further thorough imaging of different sample regions is necessary to investigate the acoustical parameters associated with the structure (check for the approximate dimensions of pore channels and windows) and also to verify the consistency of this structure through the sample height and radius.

# 4 Conclusion

A study of the sound absorption performance of a porous $Al_2O_3$/MgO sample fabricated via freeze-casting was conducted using impedance tube testing and inverse parameter fitting of the obtained surface impedance to the JCAL sound propagation model. Microstructure analysis was also conducted on the sample using Scanning Electron Microscopy and Archimedes principle. The obtained acoustical parameters showed discrepancies with the observed microstructure properties. Further investigation on the correlation of the microstructure of samples produced via freeze-casting and their sound absorption is necessary, including a analysis of the porosity throughout the height and radius of the sample.

## Acknowledgements

This work was financially supported by the Fundação de Apoio a Pesquisa do Distrito Federal (FAP-DF).

## References

[1] C. Betts, "Benefits of metal foams and developments in modelling techniques to assess their materials behaviour: a review," *Materials Science and Technology*, vol. 28, no. 2, pp. 129–143, 2012. [Online]. Available: https://doi.org/10.1179/026708311X13135950699290

[2] Y. Chen, N. Wang, O. Ola, Y. Xia, and Y. Zhu, "Porous ceramics: Light in weight but heavy in energy and environment technologies," *Materials Science and Engineering: R: Reports*, vol. 143, p. 100589, 2021. [Online]. Available: https://www.sciencedirect.com/science/article/pii/S0927796X20300474

[3] F. Han, G. Seiffert, Y. Zhao, and B. Gibbs, "Acoustic absorption behaviour of an open-celled aluminium foam," *Journal of Physics D: Applied Physics*, vol. 36, no. 3, pp. 294–302, jan 2003. [Online]. Available: https://doi.org/10.1088/0022-3727/36/3/312

[4] M. Carlesso, R. Giacomelli, T. Krause, A. Molotnikov, D. Koch, S. Kroll, K. Tushtev, Y. Estrin, and K. Rezwan, "Improvement of sound absorption and flexural compliance of porous alumina-mullite ceramics by engineering the microstructure and segmentation into topologically interlocked blocks," *Journal of the European Ceramic Society*, vol. 33, no. 13, pp. 2549–2558, 2013. [Online]. Available: https://www.sciencedirect.com/science/article/pii/S0955221913002458

[5] Z. Du, D. Yao, Y. Xia, K. Zuo, J. Yin, H. Liang, and Y.-P. Zeng, "Highly porous silica foams prepared via direct foaming with mixed surfactants and their sound absorption characteristics," *Ceramics International*, vol. 46, no. 9, pp. 12 942–12 947, 2020. [Online]. Available: https://www.sciencedirect.com/science/article/pii/S0272884220303850

[6] N. Yan, Q. Fu, Y. Zhang, K. Li, W. Xie, J. Zhang, L. Zhuang, and X. Shi, "Preparation of pore-controllable zirconium carbide ceramics with tunable mechanical strength, thermal conductivity and sound absorption coefficient," *Ceramics International*, vol. 46, no. 11, Part B, pp. 19 609–19 616, 2020. [Online]. Available: https://www.sciencedirect.com/science/article/pii/S0272884220313080

[7] C. He, B. Du, J. Ma, H. Xiong, J. Qian, M. Cai, and A. Shui, "Enhanced sound absorption properties of ceramics with graphene oxide composites," *ACS Omega*, vol. 6, no. 50, pp. 34 242–34 249, 2021. [Online]. Available: https://doi.org/10.1021/acsomega.1c03362

[8] Z. Du, D. Yao, Y. Xia, K. Zuo, J. Yin, H. Liang, and Y.-P. Zeng, "The sound absorption performance of the highly porous silica ceramics prepared using freeze casting method," *Journal of the American Ceramic Society*, vol. 103, no. 10, pp. 5990–5998, 2020. [Online]. Available: https://ceramics.onlinelibrary.wiley.com/doi/abs/10.1111/jace.17300

[9] S. Deville, "Freeze-casting of porous ceramics: A review of current achievements and issues," *Advanced Engineering Materials*, vol. 10, no. 3, pp. 155–169, 2008. [Online]. Available: https://onlinelibrary.wiley.com/doi/abs/10.1002/adem.200700270

[10] K. L. Scotti and D. C. Dunand, "Freeze casting – a review of processing, microstructure and properties via the open data repository, freezecasting.net," *Progress in Materials Science*, vol. 94, pp. 243–305, 2018. [Online]. Available: https://www.sciencedirect.com/science/article/pii/S007964251830001X

[11] N. O. Shanti, K. Araki, and J. W. Halloran, "Particle redistribution during dendritic solidification of particle suspensions," *Journal of the American Ceramic Society*, vol. 89, no. 8, pp. 2444–2447, 2006. [Online]. Available: https://ceramics.onlinelibrary.wiley.com/doi/abs/10.1111/j.1551-2916.2006.01094.x

[12] C. M. Pekor, P. Kisa, and I. Nettleship, "Effect of polyethylene glycol on the microstructure of freeze-cast alumina," *Journal of the American Ceramic Society*, vol. 91, no. 10, pp. 3185–3190, 2008. [Online]. Available: https://ceramics.onlinelibrary.wiley.com/doi/abs/10.1111/j.1551-2916.2008.02616.x

[13] Z. Xing, W. Zhou, F. Du, L. Zhang, Z. Li, H. Zhang, and W. Li, "Facile synthesis of hierarchical porous tio2 ceramics with enhanced photocatalytic performance for micropolluted pesticide degradation," *ACS Applied Materials & Interfaces*, vol. 6, no. 19, pp. 16 653–16 660, Oct 2014. [Online]. Available: https://doi.org/10.1021/am5034236

[14] H. X. Zhang, C. Z. Zhao, and C. Q. Hong, "Aligned and porous alumina ceramics prepared by camphene-based freeze-casting route: microstructure and properties," *Materials Research Innovations*, vol. 19, no. sup4, pp. S34–S38, 2015. [Online]. Available: https://doi.org/10.1179/1432891715Z.0000000001512

[15] K. Araki and J. W. Halloran, "Porous ceramic bodies with interconnected pore channels by a novel freeze casting technique," *Journal of the American Ceramic Society*, vol. 88, no. 5, pp. 1108–1114, 2005. [Online]. Available: https://ceramics.onlinelibrary.wiley.com/doi/abs/10.1111/j.1551-2916.2005.00176.x

[16] D. L. Johnson, J. Koplik, and R. Dashen, "Theory of dynamic permeability and tortuosity in fluid-saturated porous media," *Journal of Fluid Mechanics*, vol. 176, p. 379–402, 1987.

[17] Y. Champoux and J. Allard, "Dynamic tortuosity and bulk modulus in air-saturated porous media," *Journal of Applied Physics*, vol. 70, no. 4, pp. 1975–1979, 1991. [Online]. Available: https://doi.org/10.1063/1.349482

[18] D. Lafarge, P. Lemarinier, J. F. Allard, and V. Tarnow, "Dynamic compressibility of air in porous structures at audible frequencies," *The Journal of the Acoustical Society of America*, vol. 102, no. 4, pp. 1995–2006, 1997. [Online]. Available: https://doi.org/10.1121/1.419690

[19] J. F. Allard and N. Atalla, *Propagation of Sound in Porous Media: Modelling Sound Absorbing Materials*. John Wiley & Sons, Ltd, 2009.

[20] O. Umnova, K. Attenborough, and K. M. Li, "Cell model calculations of dynamic drag parameters in packings of spheres," *The Journal of the Acoustical Society of America*, vol. 107, no. 6, pp. 3113–3119, 2000. [Online]. Available: https://doi.org/10.1121/1.429340

[21] S. Gasser, F. Paun, and Y. Bréchet, "Absorptive properties of rigid porous media: Application to face centered cubic sphere packing," *The Journal of the Acoustical Society of America*, vol. 117, no. 4, pp. 2090–2099, 2005. [Online]. Available: https://doi.org/10.1121/1.1863052

[22] Y. Atalla and R. Panneton, "Inverse acoustical characterization of open cell porous media using impedance tube measurements," *Canadian Acoustics - Acoustique Canadienne*, vol. 33, 03 2005.

[23] T. G. Zieliński, "Normalized inverse characterization of sound absorbing rigid porous media," *The Journal of the Acoustical Society of America*, vol. 137, no. 6, pp. 3232–3243, 2015. [Online]. Available: https://doi.org/10.1121/1.4919806

[24] L. De Ryck, W. Lauriks, P. Leclaire, J. P. Groby, A. Wirgin, and C. Depollier, "Reconstruction of material properties profiles in one-dimensional macroscopically inhomogeneous rigid frame porous media in the frequency domain," *The Journal of the Acoustical Society of America*, vol. 124, no. 3, pp. 1591–1606, 2008. [Online]. Available: https://doi.org/10.1121/1.2959734

[25] E. Levi, S. Sgarbi, and E. A. Piana, "Acoustic characterization of some steel industry waste materials," *Applied Sciences*, vol. 11, no. 13, 2021. [Online]. Available: https://www.mdpi.com/2076-3417/11/13/5924

[26] R. Roncen, Z. E. A. Fellah, and E. Ogam, "Addressing the ill-posedness of multi-layer porous media characterization in impedance tubes through the addition of air gaps behind the sample: Numerical validation," *Journal of Sound and Vibration*, vol. 520, p. 116601, 2022. [Online]. Available: https://www.sciencedirect.com/science/article/pii/S0022460X21006131

[27] K. Levenberg, "A method for the solution of certain non-linear problems in least squares," *Quarterly of Applied Mathematics*, vol. 2, no. 2, pp. 164–168, 1944. [Online]. Available: http://www.jstor.org/stable/43633451

[28] D. W. Marquardt, "An algorithm for least-squares estimation of nonlinear parameters," *Journal of the Society for Industrial and Applied Mathematics*, vol. 11, no. 2, pp. 431–441, 1963. [Online]. Available: http://www.jstor.org/stable/2098941

[29] L. Jaouen, "Johnson-Champoux-Allard-Lafarge (JCAL) model." [Online]. Available: https://apmr.matelys.com/PropagationModels/MotionlessSkeleton/JohnsonChampouxAllardLafargeModel.html

[30] C. Hong, J. Du, J. Liang, X. Zhang, and J. Han, "Functionally graded porous ceramics with dense surface layer produced by freeze-casting," *Ceramics International*, vol. 37, no. 8, pp. 3717–3722, 2011. [Online]. Available: https://www.sciencedirect.com/science/article/pii/S0272884211003464

[31] A. Macchetta, I. Turner, and C. Bowen, "Fabrication of ha/tcp scaffolds with a graded and porous structure using a camphene-based freeze-casting method," *Acta Biomaterialia*, vol. 5, no. 4, pp. 1319–1327, 2009. [Online]. Available: https://www.sciencedirect.com/science/article/pii/S1742706108003590